



Contents lists available at ScienceDirect

## Regulatory Toxicology and Pharmacology

journal homepage: [www.elsevier.com/locate/yrtph](http://www.elsevier.com/locate/yrtph)

## Development of an integrated multi-species and multi-dose route PBPK model for volatile methyl siloxanes – D4 and D5

Tami S. McMullin <sup>a,\*,1</sup>, Yuching Yang <sup>b</sup>, Jerry Campbell <sup>b</sup>, Harvey J. Clewell <sup>b</sup>, Kathy Plotzke <sup>a</sup>, Melvin E. Andersen <sup>b</sup><sup>a</sup> Dow Corning Corporation, Health and Environmental Sciences, 2200 West Salzburg Road, Auburn, MI 48611, USA<sup>b</sup> The Hamner Institutes for Health Sciences, 6 Davis Drive, P.O. Box 12137, Research Triangle Park, NC 27709-2137, USA

## ARTICLE INFO

## Article history:

Received 19 August 2015

Received in revised form

17 December 2015

Accepted 18 December 2015

Available online xxx

## Keywords:

Octamethylcyclotetrasiloxane

Decamethylcyclopentasiloxane

D4

D5

Siloxane

PBPK

Kinetics

Risk assessment

Cyclic volatile methyl siloxane

Pharmacokinetics

Physiologically based pharmacokinetic model

## ABSTRACT

There are currently seven published physiologically based pharmacokinetic (PBPK) models describing aspects of the pharmacokinetics of octamethylcyclotetrasiloxane (D4) and decamethylcyclopentasiloxane (D5) for various exposure routes in rat and human. Each model addressed the biological and physico-chemical properties of D4 and D5 (highly lipophilic coupled with low blood: air partition coefficient and high liver clearance) that result in unique kinetic behaviors as well differences between D4 and D5. However, the proliferation of these models resulted in challenges for various risk assessment applications when needing to determine the optimum model for estimating dose metrics. To enhance the utility of these PBPK models for risk assessment, we integrated the suite of structures into one coherent model capable of simulating the entire set of existing data equally well as older more limited scope models. In this paper, we describe the steps required to develop this integrated model, the choice of physiological, partitioning and biochemical parameters for the model, and the concordance of the model behavior across key data sets. This integrated model is sufficiently robust to derive relevant dose metrics following individual or combined dermal and inhalation exposures of workers, consumer or the general population to D4 and D5 for route-to-route, interspecies and high to low dose extrapolations for risk assessment.

© 2015 The Authors. Published by Elsevier Inc. This is an open access article under the CC BY-NC-ND license (<http://creativecommons.org/licenses/by-nc-nd/4.0/>).

## 1. Introduction

Cyclic volatile methyl siloxanes (cVMSs), such as octamethylcyclotetrasiloxane (D4) and decamethylcyclopentasiloxane (D5), are low molecular weight silicones used in the manufacture of high molecular weight silicone polymers and in cosmetics and personal care products, leading primarily to low level inhalation and dermal exposures to both workers and consumers. The hazard profile of these cVMSs have been extensively evaluated (Dekant and Klaunig, 2015; in this issue; REACH, 2011a, b). To understand

the influence of kinetic factors on delivered dose of these cVMSs, our teams have conducted a comprehensive set of kinetic studies over the last several years (Tables S–1). In association with these time course data sets, we also developed several PBPK models describing the biological and physical–chemical processes regulating the kinetic disposition of either D4 or D5 in various species after different routes of exposure (Andersen et al., 2001; Reddy et al., 2003; Sarangapani et al., 2003; Reddy et al., 2007, 2008) (Tables S–2). Kinetic data and associated models were also derived to evaluate the disposition of D4 following implantation (Thrall et al., 2008) but were not used for our model development. The individual models focused on specific data sets in order to describe the kinetic behavior of either D4 or D5 in rats or humans following various routes of administration.

The first modeling work for cVMSs with D4 (Andersen et al., 2001) utilized data from a series of inhalation kinetic studies in the rat (Plotzke et al., 2000). This initial PBPK analysis uncovered a suite of processes that regulate siloxane kinetics in the rodent that

\* Corresponding author.

E-mail addresses: [tami.mcmullin@state.co.us](mailto:tami.mcmullin@state.co.us) (T.S. McMullin), [jcampbell@thehamner.org](mailto:jcampbell@thehamner.org) (J. Campbell), [hclewell@thehamner.org](mailto:hclewell@thehamner.org) (H.J. Clewell), [kathy.plotzke@dowcorning.com](mailto:kathy.plotzke@dowcorning.com) (K. Plotzke), [mandersen@thehamner.org](mailto:mandersen@thehamner.org) (M.E. Andersen).

<sup>1</sup> Colorado Department of Public Health and the Environment, 4300 Cherry Creek Drive South, Denver, CO 80246, USA.

differ from those at work with inhalation of most other volatile organic compounds. Among those characteristics were low blood: air partitioning, high fat: blood partitioning, high metabolic clearance by the liver, and slower loss of D4 from tissues than expected for simple well-mixed, flow-limited uptake compartments. In addition, a discrepancy between the rate of D4 elimination via exhalation and the associated blood levels following inhalation exposure indicated the presence of a pool of D4 in the plasma that was not available for exhalation. These observations led to inclusion of several ‘deep-tissue compartments’ to account for slow, multi-phasic loss after cessation of exposure, a pool (compartment) in blood assumed to represent lipoproteins, called a mobile lipid pool (MLP), and multiple fat compartments to describe the longer-time exhalation curves indicative of slower release of D4 from fat compartments. Sarangapani et al. (2003) expanded the Andersen et al. (2001) model to include a kinetic description of D4 following oral and dermal exposure.

D5 has even greater lipophilicity and lower blood: air partitioning than D4. Successful curve fitting with D5 time course data (Tobin et al., 2008) required addition of other deep tissue compartments, including a deep tissue store within the blood itself (Reddy et al., 2008). Thus, the rat D5 inhalation description had the largest number of tissue compartments of all the cVMSs PBPK models. The *in vitro* dermal absorption and *in vivo* dermal exposure studies in rats (Jovanovic et al., 2008) and the human volunteer inhalation studies (Utell et al., 1998) lacked the detailed tissue time courses required for establishing the presence and characteristics of deep tissue compartments. However, the dermal studies did provide information to characterize the dynamics of uptake at the skin surface while the human inhalation studies provided time-course information for metabolites to determine the pathways and time course of elimination of various low molecular weight metabolites (Utell et al., 1998). Overall the human modeling efforts for D4 and D5 adequately simulated the time-course biomarker data of D4 and D5 collected during inhalation or dermal exposure (Reddy et al., 2007).

Although each of the contributions on PBPK modeling with D4 and D5 produced good correspondence between model predictions and available data sets, the compartmental structures of these models varied according to specific data sets and the goals of model development. Unquestionably, the existence of multiple models enhances the ability to capture behaviors in the individual studies. Conversely, their proliferation presents some challenges for various risk assessment applications where it becomes difficult to determine the optimum model for estimating specific dose metrics. To improve the use of these PBPK models for risk assessment, we built a single integrated multi-compound, and multi-dose (MC-MD) route PBPK model for cVMSs that preserved the key chemical-specific biological and kinetic features determined in previous PBPK models. This contribution describes the steps required to develop this unified model, the choice of physiological, partitioning and biochemical parameters for the model, and the concordance of the model behavior across key data sets.

## 2. Methods

We used a three step process to construct a multi-compound, multi-dose route model for cVMSs that included 1) combining inhalation rodent model structures across compounds 2) coordinating model across species 3) combining routes of exposure. Table 1 shows the key model features incorporated into the current model compared to those used previously. The current computer code uses a nested algorithm to toggle specific tissues on or off depending on the chemical, the animal species and exposure route. The mass balance equations that describe the rate of change of D4

and D5 and their metabolites in various tissues are in the supplemental material (S-4). Computer code, specific scripts that reproduce all figures in this manuscript and associated documentation can be obtained from the corresponding author (TSM). The series of differential equations were solved by numerical integration using the Gear Algorithm for stiff systems in acslX version 11.8.4 (Aegis, Technologies Group, Inc, Huntsville, Alabama, USA).

### 2.1. Step 1: Combining the inhalation rodent model structures across compounds (D4 and D5)

As a first step, we developed a single compartmental suite for D4 and D5 based on inhalation exposures (Fig. 1a–d) using the structure from the rat D5 inhalation model (Reddy et al., 2008) and modified parameters and compartments for D4 based on earlier work. With D5, we retained all model features from Reddy et al. (2008) with the exception of metabolism. D4 exhibited saturable hepatic metabolism around the highest concentration (700 ppm) (Sarangapani et al., 2003). At the highest exposure concentration (160 ppm) of D5, blood concentrations were approximately 10-fold lower than D4 concentrations (Reddy et al., 2008), indicative of first-order metabolism. For the purposes of developing a common model structure across compounds, we included saturable metabolism into the D5 structure. This integrated PBPK model has six tissue compartments including blood, fat, lung, liver, slowly perfused tissues, and rapidly perfused tissues.

Physiological parameters (Table 2) such as ventilation rate [L/hr] and tissue blood flow rates (as percentage of cardiac output, L/hr) were from Brown et al. (1997). The scaling function used for the metabolism parameters and the ventilation rate was changed from  $BW^{0.7}$  to  $BW^{0.75}$  to provide consistent scaling throughout the model. Starting values for the chemical specific model parameters were adopted from the previous published models and re-parameterized, if necessary, by comparing the model simulations with experimental data. All model parameters were separately estimated for male and female with the exception of the partition coefficients. The data sets and decisions made in developing the integrated model are outlined below.

#### 2.1.1. Datasets

For both D4 and D5 kinetic studies (Plotzke et al., 2000a; Tobin et al., 2008), parent test material was synthesized with a theoretical maximum of one  $^{14}\text{C}$  radio-labeled carbon attached to each silicon atom. After exposure and tissue collection, concentrations of parent test material were measured in blood and select tissues and total radioactivity was determined in blood and the same tissues. In addition, radioactivity was measured in urine, feces, expired air and “remaining carcass.” The concentration of total metabolites was the difference between total radioactivity and the parent material concentrations.

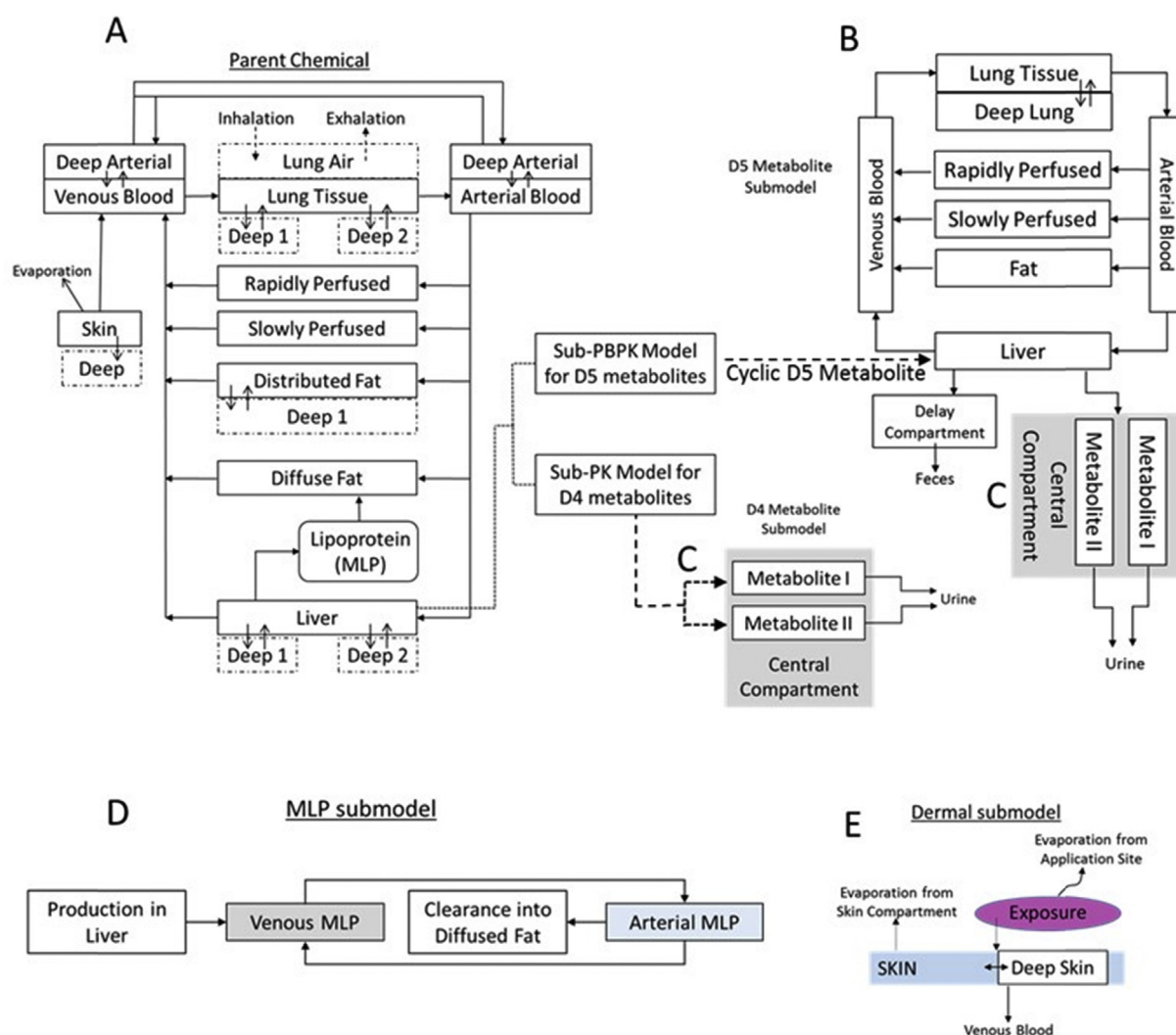
**D4:** The tissue time-course data for total radioactivity and parent chemical from  $^{14}\text{C}$ -D4 inhalation studies in male and female rats were collected following a single 6-h exposure 7, 70, or 700 ppm or multiple exposures for 6 h/day for 15 days to 7 or 700 ppm of D4 (Plotzke et al., 2000a). Exhaled breath, blood, liver, fat, lung, urine, and feces were used to construct the model. The PBPK model structure had two different fat compartments. In our current model structure, simulations for the concentration in the “distributed” fat were compared to the fat tissue data rather than the “diffuse fat” as was done previously.

**D5:** The tissue time-course data for total radioactivity and parent chemical from  $^{14}\text{C}$ -D5 inhalation studies in male and female rats were collected following a single 6-h exposure to 7 or 160 ppm or following multiple exposures (160 ppm) for 6 h/day for 15 days. The data used for determining model parameters included exhaled

**Table 1**

Comparison of the key model features in the rat reference models and the current multi-purpose rodent PBPK model.

Model compartment	Reference D4 model (Saragapani et al., 2003)	Reference D5 model (Reddy et al., 2008)	Multi-purpose PBPK model
Blood	Deep compartment in venous blood	Deep compartment in both venous and arterial blood	Adapted D5 model feature
Mobile lipid pool (MLP)	A storage depot that transports D4 from liver to diffused fat compartment in venous blood compartment	Detailed description of MLP movement from liver (via venous blood) to distributed fat (via arterial blood)	Adapted D5 model feature
Fat	Consisted of diffused and distributed fat compartments with extremely low blood flow rate to fat (<0.1% of QC)	Consisted of diffused and distributed fat compartments with literature-based blood flow rate to fat (6%)	Adapted D5 model feature
Liver	Saturable and inducible metabolism pathway	1 <sup>st</sup> order metabolism pathway	Adapted D4 model feature
Skin	Within the body (blood flow accessible)	Only considered as the top layer (a depot outside the body)	Adapted D5 model feature

**Fig. 1.** Diagram of the multi-purpose D4 and D5 PBPK model structure that describes (a) the time –course tissue concentrations of D4 and D5 (b) hydroxylated D5 metabolite sub-model (c) short chain silanol metabolite sub-model (d) production and distribution of the mobile lipid pool (e) dermal uptake of D4 and D5 in humans.

breath, tissues of blood, liver, fat, and lung, urine, and feces (Tobin et al., 2008).

### 2.1.2. Model structure and parameter estimation

Physiological values used in the model are listed in Table 2. Model parameter values for D4 and D5 are listed in Tables 3 and 4.

**Blood:** The blood compartment description from Reddy et al. (2008) was retained. The plasma compartment was converted to

a blood compartment containing both arterial and venous blood. Each of these compartments has a deep compartment (see deep tissue compartment description below).

**Liver and Mobile Lipid Pool:** A ‘mobile lipid pool’ (MLP) compartment describes the transport of a bound form of D4 and D5 that is formed in the liver, transported from the liver to the venous blood as “venous blood MLP” and then enters the arterial blood as “arterial blood MLP” via flow-limited transport. The arterial blood

**Table 2**

Physiological parameters for cyclic siloxane multi- purpose PBPK model.

Physiological parameter <sup>a</sup>		Rat	Human
Tissue volumes (fraction of BW)			
Body weight (kg)	BW (kg)	0.185	70
Blood	VBLDc	0.074	0.079
Diffuse fat	VFATDIFFc	0.063	0.214
Distributed fat <sup>c</sup>	VFATDISTc	0.007	0.000
Liver	VLIVc	0.034	0.026
Lung	VLNGc	0.005	0.008
Rapidly perfused	VRAPc	0.100	0.080
Slowly perfused	VSLWc	0.627	0.437
Blood Flows (fraction of QCC)			
Cardiac output	QCC [L/hr/kg <sup>0.75</sup> ]	15	Varies <sup>b</sup>
Alveolar ventilation	QPC [L/hr/kg <sup>0.75</sup> ]	15	Varies <sup>d</sup>
Diffuse fat	QFATDIFFc	0.063	0.052
Distributed fat <sup>c</sup>	QFATDISTc	0.007	0.000
Liver	QLIVc	0.183	0.227
Rapidly perfused	QRAPc	0.411	0.472
Slowly perfused	QSLWc	0.336	0.249

<sup>a</sup> All physiological parameter values obtained from Brown et al. (1997).<sup>b</sup>  $(-6.85 * \log_{10}(\text{Age}) + 16.8) * 60.0$ .<sup>c</sup> Distributed fat turned off for humans.<sup>d</sup> Study specific based on measured values (Utell et al., 1998).**Table 3**

D4 specific parameters for Cyclic Siloxane Multi-Purpose PBPK Model.

D4 specific parameters <sup>a</sup>		Rat		Human	
<i>Partition Coefficients (unitless)</i>					
Blood:air	PBld	0.85		0.96	
Diffuse fat:air	PFatDiffAir	600		600	
Distributed fat:air	PFatDistAir	100		NA	
Liver:air	PLivAir	21.2		21.2	
Lung:air	PLngAir	7.84		7.84	
Rapidly perfused:air	PRapAir	8.47		8.47	
Slowly perfuse:air	PSlwAir	8.47		8.47	
<i>Diffusion Coefficients (unitless)</i>		<b>Male</b>	<b>Female</b>	<b>Male</b>	<b>Female</b>
Diffuse fat	PermFatDiff	0.4	0.5	1	1
Distributed fat	PermFatDist	0.3	0.3	NA	NA
Slowly perfused	PermSlw	1	1	0.045	0.045
<i>Metabolic Parameters</i>					
Maximal capacity	Vmax[mg/hr/BW <sup>0.75</sup> ]	3.08	3.08	62	62
Affinity constant	Km [mg/L]	0.5	0.5	10	10
<i>Mobile Lipid Pool (MLP) Parameters [1/hr]</i>					
Production rate of MLP	KMLP	0.0408	0.03	3.78	3.78
Clearance from MLP compartment	Kremoval	0.055	0.1	0.39	0.39
<i>Mass Transfer Parameters for Deep Compartments [1/hr]</i>					
Into deep arterial blood	kArtBldDeepIn	NA	NA	NA	NA
Out of deep arterial blood	kArtBldDeepOut	NA	NA	NA	NA
Into deep venous blood	kVenBldDeepIn	NA	NA	NA	NA
Out of deep venous blood	kVenBldDeepOut	NA	NA	NA	NA
Into 1st deep lung compartment	kLngDeep1In	0.018	0.0075	5.0	5.0
Into 2nd deep lung compartment	kLngDeep2In	NA	NA	0.001	0.001
Out of 1st deep lung compartment	kLngDeep1Out	0.0166	0.02	NA	NA
Out of 2nd deep lung compartment	kLngDeep2Out	NA	NA	NA	NA
Into 1st deep liver compartment	kLivDeep1In	0.0006	0.0006	0.55	0.55
Into 2nd deep liver compartment	kLivDeep2In	NA	NA	NA	NA
Out of 1st deep liver compartment	kLivDeep1Out	0.009	0.009	0.13	0.13
Out of 2nd deep liver compartment	kLivDeep2Out	NA	NA	NA	NA
Into deep fat compartment	kFatDeepIn	NA	NA	0.23	0.23
Out of deep fat compartment	kFatDeepOut	NA	NA	0.11	0.11
<i>Dermal Absorption Rate Constants</i>					
Evaporation from skin surface	kEvapC [mg/hr-cm <sup>2</sup> ]	NA	NA	9.0	9.0
Evaporation from skin tissue	kSknOutC [1/hr]	NA	NA	380.0	380.0
Absorption rate from skin surface to skin tissue	kSknIn [mg/hr-cm <sup>2</sup> ]	NA	NA	200.0	320.0
Absorption rate from skin to blood	kSknBld [1/hr]	NA	NA	0.045	0.045

<sup>a</sup> Source of parameter (experimental or model derived) and parameterization process for each parameter is discussed in detail in the text.

MLP transfers into the diffuse fat compartment (Fig. 1d). This pool of D4 and D5 is distinct from the free circulating concentrations of D4 and D5; it is unavailable for exhalation, metabolism and

equilibration with tissues. The “MLP” likely represents cVMS associated with circulating lipids, such as lipoproteins and transported in the body with these lipids (Looney et al., 2000; Andersen



**Table 4**

D5 specific parameters for Cyclic Siloxane Multi-Purpose PBPK model.

D5 specific parameters <sup>a</sup>		Rat		Human	
Parameter					
<i>Partition Coefficients (unitless)</i>					
Blood:air	PBLD	0.55		0.5	
Diffuse fat:air	PFATDIFFAIR	1436		1436	
Distributed fat:air	PFATDISTAIR	1436		1	
Liver:air	PLIVAIR	11.1		11.1	
Lung:air	PLNGAIR	45.36		45.36	
Rapidly perfused:air	PRAPAIR	3.4		3.4	
Slowly perfuse:air	PSLWAIR	7		7	
<i>Diffusion Coefficients (unitless)</i>					
Diffuse fat	PERMFATDIFF	0.026	0.027	1	1
Distributed fat	PERMFATDIST	0.02	0.03	NA	NA
Slowly perfused	PERMSLW	0.05	0.06	1	1
<i>Metabolic Parameters</i>					
Maximal capacity	V <sub>max</sub> [mg/hr/BW <sup>0.75</sup> ]	30	20	11	10
Affinity constant	K <sub>m</sub> [mg/L]	20	20	10	10
<i>Mobile Lipid Pool (MLP) Parameters [1/hr]</i>					
Production rate of MLP	KMLP	4	3	3.0	2.0
Clearance from MLP compartment	Kremoval	2.0	1.7	1.0	0.5
<i>Mass Transfer Parameters for Deep Compartments [1/hr]</i>					
Into deep arterial blood	kArtBldDeepIn	0.0016	0.0026	NA	NA
Out of deep arterial blood	kArtBldDeepOut	0.006	0.003	NA	NA
Into deep venous blood	kVenBldDeepIn	0.0016	0.0026	NA	NA
Out of deep venous blood	kVenBldDeepOut	0.006	0.003	NA	NA
Into 1st deep lung compartment	kLngDeep1In	0.6	0.05	3	4
Into 2nd deep lung compartment	kLngDeep2In	0.001	0.001	NA	NA
Out of 1st deep lung compartment	kLngDeep1Out	0.6	0.6	1	0.0708
Out of 2nd deep lung compartment	kLngDeep2Out	0.007	0.007	NA	NA
Into 1st deep liver compartment	kLivDeep1In	0.15	0.5	2.17	0.438
Into 2nd deep liver compartment	kLivDeep2In	0.004	0.003	NA	NA
Out of 1st deep liver compartment	kLivDeep1Out	0.2	0.5	0.0508	0.195
Out of 2nd deep liver compartment	kLivDeep2Out	0.003	0.006	NA	NA
Into deep fat compartment	kFatDeepIn	NA	NA	NA	NA
Out of deep fat compartment	kFatDeepOut	NA	NA	NA	NA
<i>Dermal Absorption Rate Constants</i>					
Evaporation from skin surface	kEvapC [mg/hr-cm <sup>2</sup> ]	NA	NA	4.26	4.26
Evaporation from skin tissue	kSknOutC [1/hr]	NA	NA	0.43	0.498
Absorption rate from skin surface to skin tissue	kSknInC [mg/hr-cm <sup>2</sup> ]	NA	NA	105.09	180.0
Absorption rate from skin to blood	kSknBld [1/hr]	NA	NA	0.0009	0.00065

<sup>a</sup> Source of parameter (experimental or model derived) and parameterization process for each of parameter is discussed in detail in the text.

et al., 2001; Sarangapani et al., 2003; Reddy et al., 2008).

The time-course concentrations of the parent chemical and the metabolites in the liver, blood, and urine were used to estimate the MLP parameters. The initial production and clearance rate constants of the MLPs were from Sarangapani et al. (2003) and Reddy et al. (2008) and these parameters were converted into the appropriate units for this current model. The MLP clearance rate (1/hr) in our model (K<sub>removal</sub>) was calculated from CL<sub>mlp</sub> (clearance rate [L/hr]) used in the Reddy et al. (2008) D5 rat inhalation model as follows:

$$K_{\text{removal}} = (Q_{\text{fat}} \cdot \text{CL}_{\text{MLP}}) / (Q_{\text{fat}} + \text{CL}_{\text{MLP}}) / V_{\text{ArtBld}}$$

MLP parameter values for this model were then manually optimized to fit the single-exposure experimental data.

**Fat:** The description of various fat tissues was also from Reddy et al. (2008). There are two compartments representing separate types of fat: distributed and diffuse fat. The distributed fat represents depots, such as perirenal or abdominal fat that are readily identifiable in the body. The diffuse fat compartment represents depots that are more widely distributed in multiple tissues throughout the body. Initial values for fat tissue parameters were taken from the original models and optimized by visual comparisons of the simulated D4 or D5 concentration in the distributed fat compartment to the measured fat concentration.

**Deep Tissue Compartments:** The previously developed rat models

had “deep compartments” to describe the time-course kinetic behavior of the cVMSs in the lung, liver, fat and blood compartments over longer periods of exposure and observation. These deep tissue compartments represent storage depots from which the free parent chemical is released first to the tissues themselves and then to systemic circulation (Reddy et al., 2008). They were included because the more conventional one-compartment descriptions of these tissues did not adequately reflect tissue time course after exposures. D4 and D5 move between the tissue compartments and deep compartments by diffusional transport. Due to its higher lipophilicity, fitting the tissue data time courses for D5 required two sequential deep compartments in the lung and liver. In the integrated model these additional deep compartments toggle off when simulating D4 kinetics. This diffusion description was changed from a concentration based compartment used in the Reddy et al. (2008) model to a mass based compartment to avoid the need to include an estimate of the volume of tissue deep compartments. The parameter values from the Reddy et al. (2008) model were kept constant in our model. Reddy et al. (2008) provides a detailed description of the parameterization process used to obtain the deep tissue compartment rate constants.

**Metabolism:** Hepatic metabolism of D4 and D5 occurs by methyl group-oxidation, rearrangement of the subsequent Si –CH<sub>2</sub>OH to SiOCH<sub>3</sub> followed by hydrolysis with ring opening to produce a series of linear silanols that are excreted into the urine. Inducible metabolism of D4 saturates at higher doses in the male rat and

follows Michaelis–Menten (M–M) kinetics. However, the hepatic metabolism of D5 was linear at the exposure levels evaluated in the kinetic rodent studies. This current multi-compound model incorporates saturable M–M kinetics for both D4 and D5; however, based on the  $K_m$  values for binding, D5 metabolism is always in a linear range even in the rat.

The time-course concentrations of the parent chemical and the metabolites in the liver, blood, and urine were used to estimate metabolic constants for this model. The work on D4 by Sarangapani et al. (2003) and D5 by Reddy et al. (2008) provided initial values for these parameters. Reddy et al. (2008) described D5 metabolism with a first order rate constant,  $k_{met}$  where  $k_{met} = V_{max}/K_m$ . We used a sequential parameterization process to determine the maximum metabolic rate constant ( $V_{max}$ ) and the Michaelis–Menten constant ( $K_m$ ) from the first-order rate constant. We ran the Reddy D5 model at 160 ppm (the highest exposure concentration) to obtain the peak concentration of free D5 in venous blood leaving the liver, a concentration approaching maximal velocity of the enzyme ( $V_{max}$ ). We then set  $K_m$  to a value approximately 50 times higher than the simulated  $CV_{liv}$  from 160 ppm exposure to estimate  $V_{max}$ . After fitting to estimate  $V_{max}$ ,  $K_m$  was estimated using the equation  $V_{max}/K_m = k_{met}$ . Final metabolism parameters were then adjusted to provide a good visual representation of the time course data for tissues and metabolites.

**Metabolites:** A compartmental model with two first-order clearance rates was used to describe the distribution and urinary elimination of a bulk pool of short chain silanol metabolites (Fig. 1c). Final model parameters were determined by visual optimization using the blood time-course data for the total metabolites following a single 6-h inhalation exposure to 160 ppm D5 or 7, 70 and 700 ppm D4.

D5 metabolism produces a lipophilic cyclic metabolite, presumably hydroxyl-D5, which has a methyl group replaced by a hydroxymethyl or methoxy group. A five-compartment metabolite model adapted from the D5 rat inhalation model was included in our integrated model to simulate concentrations of this metabolite in plasma, selected tissues and urine (Fig. 1b). In the sub-model for the metabolite, the cyclic D5 metabolite undergoes further metabolism to produce linear silanols of variable chain length similar to D4.

**Partition coefficients:** Various approaches were used previously to derive tissue/blood partition coefficients (PCs) for D4 and D5. For the combined model, the partition coefficients for D4 were mainly adapted from Sarangapani et al., 2003. Initial estimates of the tissue: blood PC's were first derived based on *in vitro* measurements and subsequently re-optimized to describe the *in vivo* data (Sarangapani et al., 2003). For D5, the values of tissue/blood PCs were calculated by dividing the tissue/air PCs by the model estimated *in vivo* blood/air PCs. This approach results in a slightly higher blood/air coefficient (0.5 for rat) while conserving the tissue/blood relationship observed of the *in vitro* estimation.

## 2.2. Step 2: Coordinating models across species (rodent to human)

We next combined the rodent and human models into a single model structure. We first compared the rodent model structure (from Step 1) to the existing D4 and D5 human inhalation PBPK model structures (Reddy et al. 2003, 2008). The previous human models describe the kinetic disposition of inhaled D4 and D5 in humans with six compartments, incorporation of a MLP pool and chemical specific deep tissue compartments. The original descriptions used only one deep compartment to describe the liver and the lung tissue concentrations and a single compartment to describe fat concentrations. This lumping approach was a result of the limited human tissue data (plasma, exhaled breath, and urine)

from which the model could be developed (Tables S–1). The steps in modifying the human models (Reddy et al. 2003, 2008) were similar to those taken with the rodent models. These changes include conversion of the plasma compartment to a blood compartment, use of mass-based parameters to describe kinetics in the deep tissue compartments, and saturable liver metabolism (Table 1). The original D4 human inhalation model (Reddy et al., 2003) did not have a lung compartment. The integrated model has a deep lung compartment in order to describe D5 tissue time courses but is toggled off for D4 simulations. The chemical specific metabolite sub-model for humans was the same as that used in the rodent model.

### 2.2.1. Datasets

**D4:** Six male volunteers were exposed to 10 ppm vapor of  $^{14}C$ -D4 for 1 h while performing intermittent exercise (Utell et al., 1998). Total radioactivity was determined for blood, exhaled breath, and urine samples. Blood samples were collected during and after exposure up to 24 h post-exposure. Exhaled breath samples were collected up to 72 h after the cessation of the exposure. Urine samples were collected up to 7 days post-exposure. Individual silanol metabolites were measured in these urine samples.

**D5:** Three male and two female volunteers were exposed to D5 vapor at 10 ppm for 1 h (Plotzke et al., 2002). During the exposure, subjects performed intermittent exercise, alternating rest and exercise periods on a regular interval. The corresponding changes in the ventilation rate and the minute volume were recorded. Blood and exhaled breath samples were collected during the exposure and the post-exposure period up to 24 h after the cessation of the exposure.

### 2.2.2. Parameter estimation

The physiological values for tissue volumes and blood flow rates for humans were from the literature and presented in Table 2. Model parameter values for D4 and D5 are listed in Tables 3 and 4.

**Partition coefficients:** Human blood: air PCs for D4 and D5 were estimated by visual optimization of the model PCs to the individual human data from the inhalation study. The human tissue: air PCs for D4 and D5 were the same as used in the current rat models. This decision resulted in greater values for PC tissue: air for the liver and slowly perfused compartments compared to the values used in the earlier PBPK models. The tissue: blood PCs for the current human model were calculated from the following ratios:

$$\text{Tissue : blood} = \text{rat PC tissue : air} / \text{model estimated PC blood : air}$$

**Metabolism:** Individual human M–M metabolic parameters for D4 and D5 were estimated as done for the rat D5 metabolic parameters. D5 individual human blood and exhaled breath data and D4 blood, exhaled breath and urine data were used to obtain estimates for each of the individuals.  $V_{max}$  was adjusted based on individual data while setting  $K_m$  to a sufficiently high value to ensure linear kinetics. After estimating values of these parameters for individual volunteers, these values were averaged to obtain a single human value for simulating averaged population data.

**Metabolite Sub-Model:** The parameters for the D4 and D5 metabolite sub-model were adapted from the combined rat model from Step 1.

**Mobile Lipid Pool:** MLP parameters for D4 and D5,  $K_{mlp}$  and  $K_{removal}$ , were visually optimized using the individual blood and exhaled breath concentrations. Parameters for individuals were then averaged to obtain the corresponding population parameters.

**Deep Compartments:** Deep compartments and associated

parameters used in the original human models for D4 and D5 were retained in the current structure (Fig. 1). The D5 model structure has blood, lung and liver deep compartments. The Reddy et al. (2003) model for D4 only included a deep fat compartment. Simulation of the human D4 data sets with inclusion of a deep liver compartment improved the model fit to the data and therefore, the deep liver compartment was retained in the unified D4 model.

The mass-transfer coefficients for the slowly perfused and deep compartments were initially optimized using individual blood and exhaled breath data in individuals and then the averaged individual parameter values for D5 were successfully used to simulate the blood and exhaled breath data at the population level. Simulation of the D4 time-course data at the population level, however, required re-optimization of the final populations level parameter values.

### 2.3. Step 3: Combining routes of exposure (inhalation and dermal)

We next added the dermal route of exposure for humans using the same dermal sub-model structure for D4 and D5 as was used in Reddy et al. (2007) (Fig. 1e). Two processes regulate absorption of cVMSs from the skin surface: absorption from the application site to the skin tissue and evaporation of cVMSs from the skin surface at the site of application. Upon absorption into the skin, cVMSs either transfer into the venous blood for systemic distribution or are retained in a deep skin compartment with transfer back to the skin compartment for either absorption to blood or evaporation to air.

#### 2.3.1. Datasets

<sup>13</sup>C-labeled D4 (Plotzke et al., 2000a, b) or D5 (Plotzke et al., 2002) was applied to the axillae of three male and three female subjects. A total of 1.4 g (males) or 1.0 g (females) was split equally between both axillae. The material was allowed to absorb and evaporate for 5 min. Blood and exhaled air samples were collected over various time periods before and after the exposure.

#### 2.3.2. Parameter estimation

We estimated skin-specific rate constants using the dermal-only dataset with other model parameters identical to those used for inhalation. The evaporation rates ( $K_{\text{evpc}}$ ) for D4 (Table 3) and D5 (Table 4) were experimentally derived *in vitro*. The remaining skin compartment parameters were based on visual optimization of the model simulation to the dermal exposure data for blood and exhaled breath concentrations.

### 2.4. Sensitivity analysis

We conducted a sensitivity analysis of the D4 and D5 model for rat (inhalation) and human (inhalation and dermal). Sensitivity was assessed in the rat using a single 6 h exposure to either D4 or D5 at 7 ppm while the human was evaluated using the human the exposure scenarios presented in Figs. 5 and 6. The average blood concentration over a 24 h timeframe (calculated as AUC/Time) for each siloxane and exposure scenario was used to assess the importance of specific parameters on the most likely dose metric for cross-species extrapolation to evaluate points of departure. Normalized sensitivity coefficients (fractional change in output divided by fractional change in input) were calculated with the forward difference method. Changes in the average blood concentration for either D4 or D5 were calculated for 1% changes of each parameter. A parameter was deemed sensitive if the resulting coefficient was >0.10 in absolute value. Only parameters meeting the sensitivity cutoff for at least one endpoint are presented in the results.

## 3. Results

### 3.1. Model evaluation

We developed a single MC-MD route PBPK model for cVMSs (Fig. 1) using a nested approach that built upon an original D5 rodent model structure. The current rat model structure describes the time-course concentrations of total radiolabeled and parent D4 and D5 in exhaled breath, blood, tissues and urine during and following a both single (Fig. 2) and multiple (Fig. 3) exposure levels at several concentrations using a consistent set of chemical and species specific parameters (Tables 3 and 4). To ensure consistency between this combined multi-compound, multi-dose model and the original D4 and D5 models, the simulated time-averaged plasma and liver concentrations in the rat following 160 ppm D5 and 700 ppm D4 were compared with the simulation results from the original PBPK models (results not shown). Although no formal statistics were applied for curve fitting, this integrated, MC-MD model did as well as the earlier model bespoke models in describing the diverse data sets underpinning model development.

The richness of the time-course kinetic data with these siloxanes and their unusual distributional characteristics - extremely high blood clearance of free chemical and high fat: blood partitioning - have provided a rare opportunity to better understand the distribution of lipophilic compounds into body compartments. With most moderately lipophilic compounds, lower clearance and more modest fat: blood partitioning, obscure the kinetic processes associated with loss of compounds from tissue after cessation of inhalation. The observations of slower release than expected from simple, one-compartment depictions of tissues with these siloxanes is simply indicative of more physiologically-realistic disposition of lipophilic compounds into cells that are themselves comprised of diverse intracellular compartments - endoplasmic reticulum, mitochondria, nucleus/nucleolus, liposomes, and lysosomes, etc. - all surrounded by lipid based membranes. Our multi-compartment fat depots in tissues such as lung and liver likely represent differential diffusional characteristics into and out of these intracellular lipid pools. This same behavior should occur with other compounds. Time course studies for kidney, liver, lung, etc. with other moderately lipophilic volatiles, such as styrene, could be mined to evaluate multi-compartment tissue structures with a more diverse group of compounds.

cVMSs are extensively cleared from the body by exhalation of free parent material (equivalent to total radioactivity in exhaled breath; Fig. 2b, e; Fig. 3c, g) and hepatic metabolism leading to various polar silanols (Varaprath et al., 1999, 2003). As became apparent through the previous modeling efforts, measured plasma concentrations of parent cVMSs represent both a bound, sequestered pool of siloxane and a free, circulating portion of the siloxane that is available for distribution to other tissues and for exhalation from the lung (Fig. 4c, d). In our MC-MD model, the unavailable pool of material in the MLP compartment is presumed to be blood lipids. Identification of the MLP pool as the most likely carrier remains a strong hypothesis that will benefit from more detailed analysis of siloxanes in various components of plasma.

Our MC-MD model has dose-dependent, saturable hepatic metabolism and simulates the time-course concentrations of both parent siloxane and total silanol metabolites separate from total radiolabeled equivalents (Fig. 4a, b). For D5, the model equations capture both circulating blood and tissue concentrations of the hydroxylated D5 metabolite (data not shown). Urinary time-course data for individual silanols metabolites were included in the first human PBPK model by Reddy et al. (2003) and compared to urinary time course data from the volunteers. Further time course studies of plasma and/or urinary concentrations of individual silanols

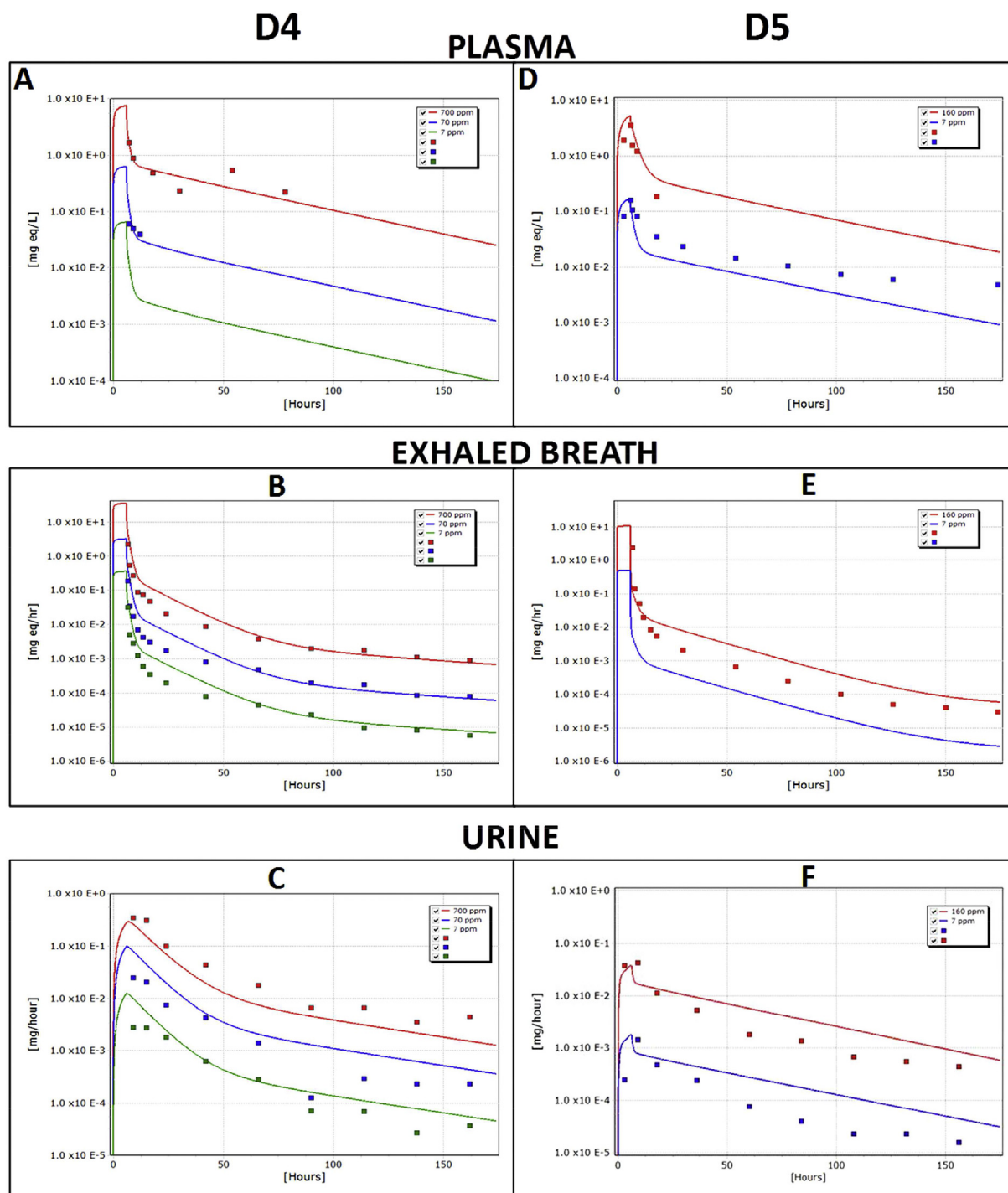


**Fig. 2.** Data (symbols) and model simulations (lines) of time-course concentrations of parent D4 in (A) plasma (B) rate of total amount of radiolabeled equivalents of D4 in exhaled breath (equivalent to parent D4 for exhaled breath. Parent accounted for all radioactivity) and (C, F) rate of amount radiolabeled equivalents of D4 in urine following a single 6-h inhalation exposure of male rats to 700, 70 or 7 ppm D4. (D) Plasma concentration (E) rate of total amount of radiolabeled equivalents of D5 in exhaled breath and (F) rate of amount radiolabeled equivalents of D5 in urine following a single 6-hr inhalation exposure of male rats to 7 and 160 ppm D5.

would be necessary to expand the current integrated model to describe the kinetic behavior of individual silanol metabolites, such as dimethylsilanediol (DMSD), across compounds and exposure routes in rodents.

The next step in developing the MC-MD model structure built on the rat model to describe the kinetic behavior of the cVMSs in humans following inhalation exposure. The interspecies extension to the MC-MD model adequately described both individual (data

not shown) and population time-course data of total D4 in exhaled breath, plasma (Fig. 5a, b) and total D5 in exhaled breath and plasma (Fig. 6a, b) following inhalation exposure. Compared to the original human inhalation model code a deep lung, fat and liver compartment were included in the human MC-MD model to maintain consistency across species. Although the amount of D4 in the deep liver compartment was very small in the MC-MD model simulations, inclusion of this compartment improved the visual fit



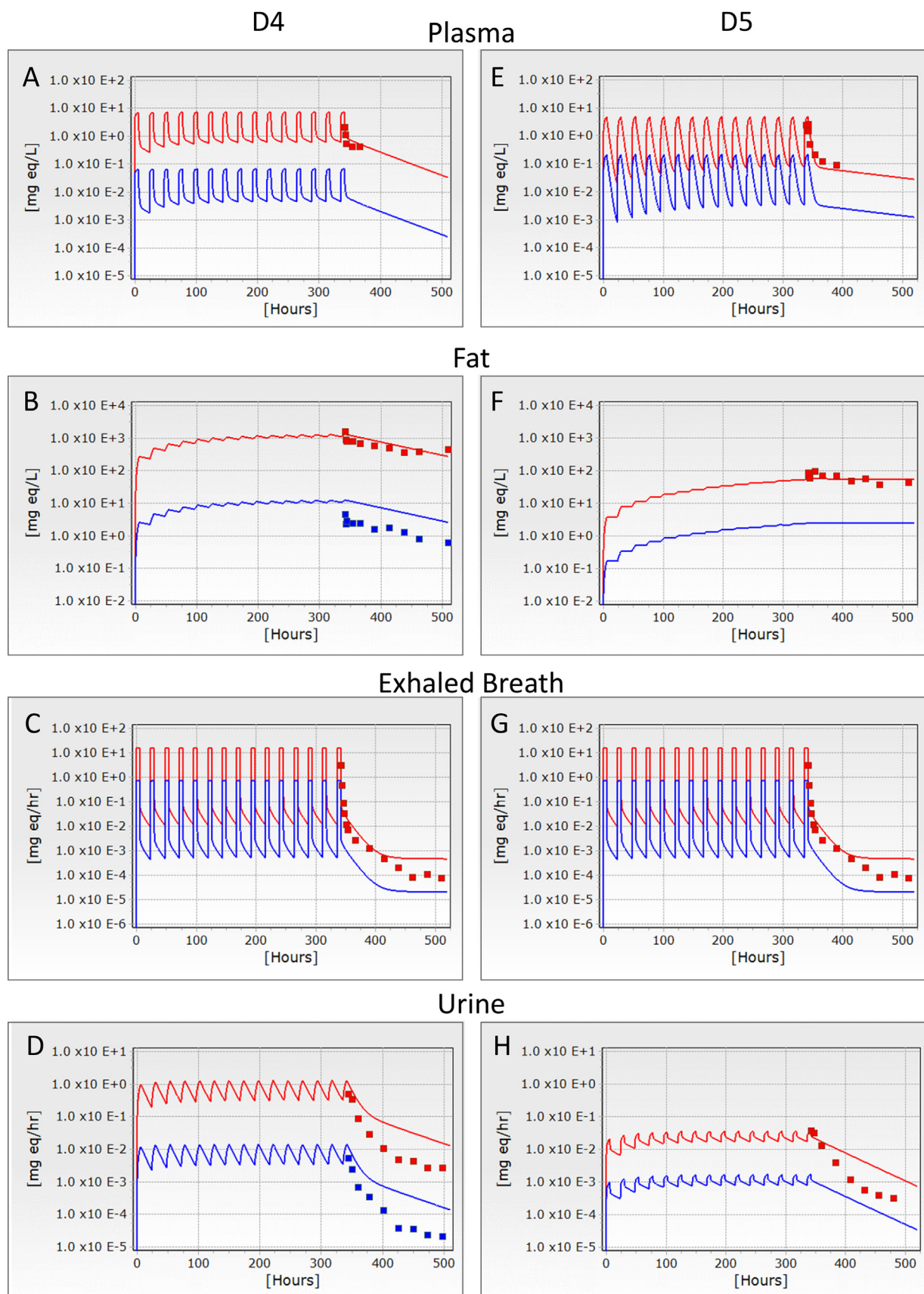


**Fig. 3.** Data (symbols) and model simulations (lines) of time-course concentrations of parent D4 in (A) plasma and (B) fat (C) rate of total amount of radiolabeled equivalents of D4 in exhaled breath and (D) rate of amount radiolabeled equivalents of D4 in urine following 15 days of inhalation exposure of male rats to 700, 70 or 7 ppm D4. (E) Plasma and (F) fat concentrations (G) rate of total amount of radiolabeled equivalents of D5 in exhaled breath and (H) rate of amount radiolabeled equivalents of D5 in urine following 15 days of inhalation exposure of male rats to 7 or 160 ppm D5.

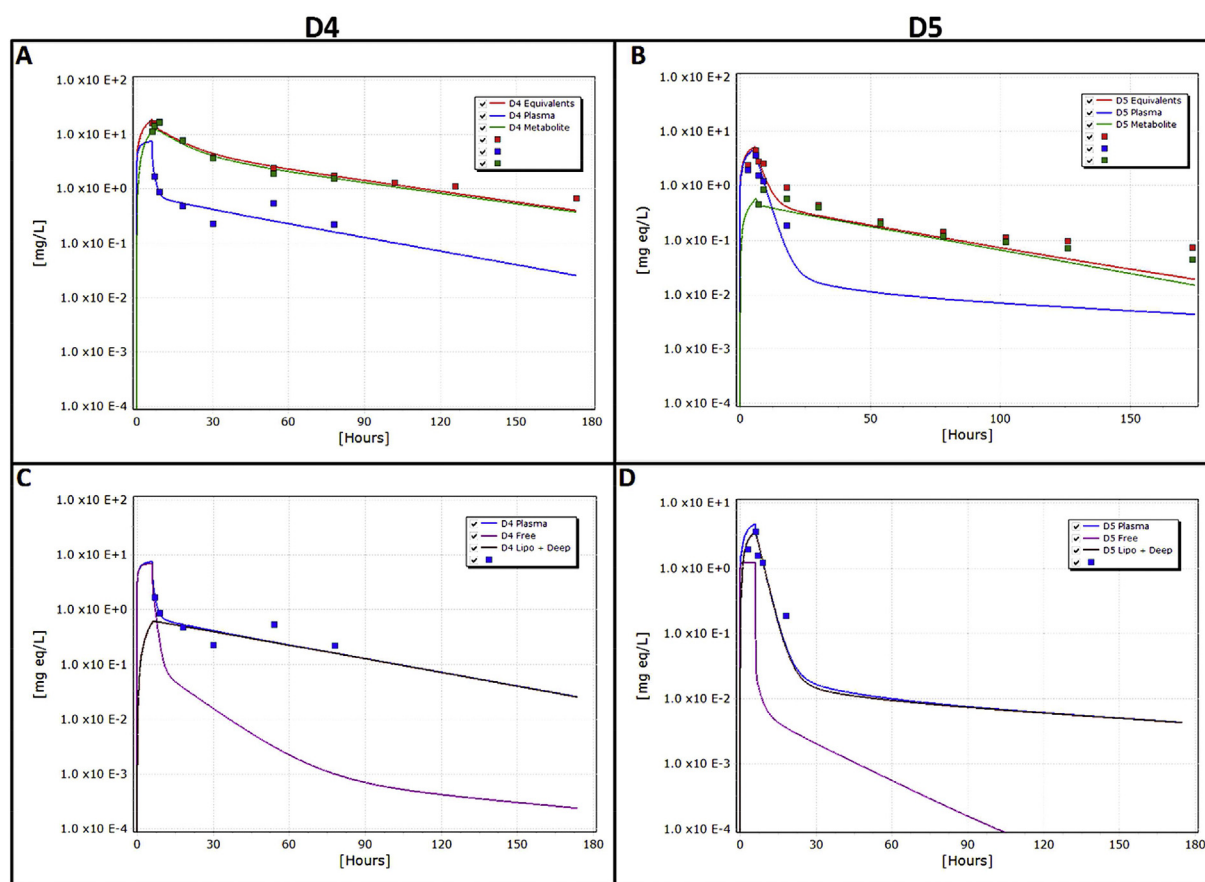


**Fig. 4.** Data (symbols) and model simulations (lines) of the time-course plasma concentrations of total radiolabeled equivalents (red), parent siloxane (blue) and calculated concentrations of metabolites (green) in male rats following a single 6-h inhalation exposure to (A) 700 ppm D4 or (B) 160 ppm D5. Measured plasma concentrations of parent siloxane shown in A and B (blue) represent the lipid bound material and the free, circulating material available for distribution to other tissues and exhalation from the lung for (C) D4 or (D) D5.

of exhaled air data during the 2-h period immediately following termination of exposure while having no effect on simulations of the urine or blood data.

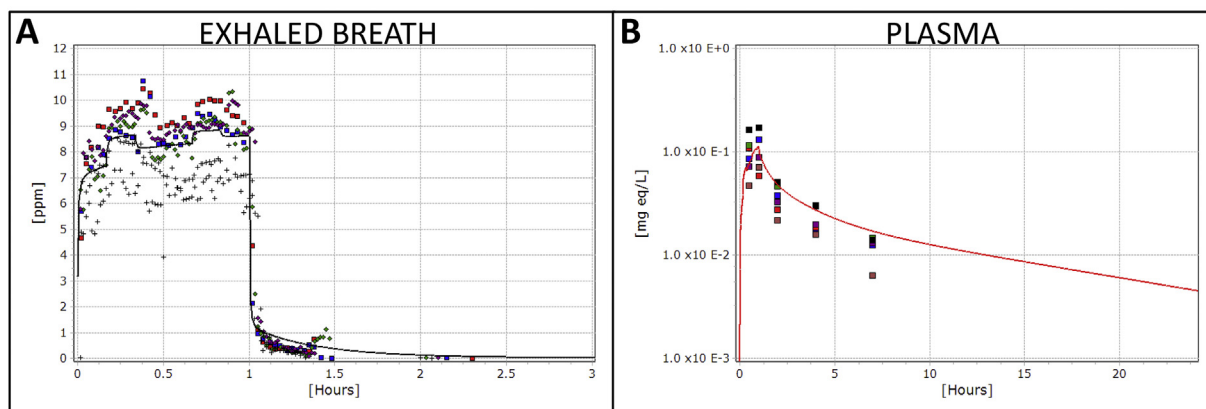
The dermal exposure route was added after finalizing the inhalation model structure and its parameterization. Based on the wealth of data available for dermal exposures from *in vitro* and *in vivo* human skin studies and *in vivo* rodent studies, modeling of the dermal uptake had three compartments - a skin surface depot, a skin tissue compartment from which compound could transfer back to the skin or move into either a deep tissue compartment or to the venous blood and the deep tissue storage compartment of the skin. The deep compartment likely represents siloxanes retained in the stratum corneum that are then slowly released into the viable epidermis and bloodstream upon termination of exposure (Reddy et al., 2007). Upon termination of exposure, cVMSs in the viable epidermis can either diffuse into blood or back to the skin surface for evaporation. While this description was essential to capture the time-course behavior of cVMSs following dermal application, the specific depots in the skin during absorption and the period of persistence in skin over the 24 h are not absolutely well-defined. The skin-specific uptake parameters were estimated using the dermal-only dataset while keeping all other model parameters determined from the fitting of the inhalation studies constant at the population-level. We also note that the dermal studies were with axilla skin that absorbs chemicals more rapidly than other skin areas. Absorbed dose and circulating cVMS concentrations are expected to be lower for siloxane exposures to other skin surfaces. Overall, the integrated MC-MD PBPK model for

cVMSs simulated D4 and D5 time-course exhaled breath, blood and various tissues data following the application of pure D4 (Fig. 5c, d) or D5 (Fig. 6c, d) onto the axilla skin.

### 3.2. Sensitivity analysis

The normalized sensitivity coefficients for sensitive parameters in at least one of the scenarios are shown in Tables S–3. Similar results were seen between the rat and human for both D4 and D5 regardless of exposure route. The most sensitive parameter across species and dose routes on the average blood concentration was the blood: air partition coefficient which was experimentally determined. This was followed by parameters related to the disposition of siloxane in within the lipid handling system which includes the liver (KMLP) and fat (KREMOVAL) and metabolic rates which were estimated to fit either the time-course concentration of parent chemical in liver and fat or the difference between parent and total radioactivity in liver and plasma. The rate constants for deep compartments (liver and blood) showed limited sensitivity and only in the human inhalation scenarios. Physiological parameters including BW, cardiac output, fraction of blood flow to liver fat, rapidly and slowly perfused tissues as well as the fraction of BW represented by blood and liver were sensitive for average blood concentration. For the dermal exposure scenario, additional parameters related directly to the uptake of siloxane including the dermal surface area exposed (DERMAREA1 and 2) and the penetration rate into stratum corneum (KSKINC) and from skin tissue to skin blood (KSKNBLD).

## INHALATION



## DERMAL

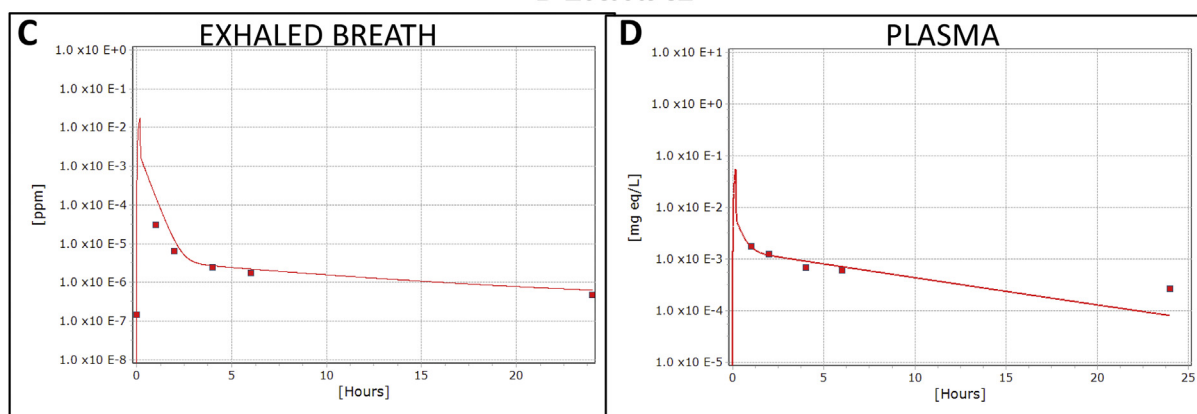


**Fig. 5.** Model simulation (lines) and data (symbols) (mean  $\pm$  SD;  $n = 5$ ) of D4 in (A) exhaled breath and (B) plasma in male volunteers during and following 10 ppm D5 vapor exposure for 1-h or (C) exhaled breath and (D) plasma during and following a single application of 1.4 g  $^{13}\text{C}$ -D4 to skin axilla.

### 4. Discussion

The main purpose of developing this integrated MC-MD PBPK model was to provide a single model construct for use in risk assessment applications for either D4 or D5 and to be able to compare the kinetic disposition between these cVMSs. The process of developing an integrated, multi-compound, multi-route, multi-species PBPK model for D4 and D5 uncovered important questions and challenges to consider when combining several customized models into a single model suitable for risk assessment purposes. Selection of the appropriate datasets to optimize the model parameters from an extensive body of kinetic studies (Table 1) was the most critical decision for this process. To achieve this overall purpose, individual model parameter values were optimized to the datasets that were the most informative of the various underlying kinetic processes regulating those parameters. In general, the preferred data sets were from rats because they had more extensive time-course data and included detailed collection of tissues at various times post-exposure.

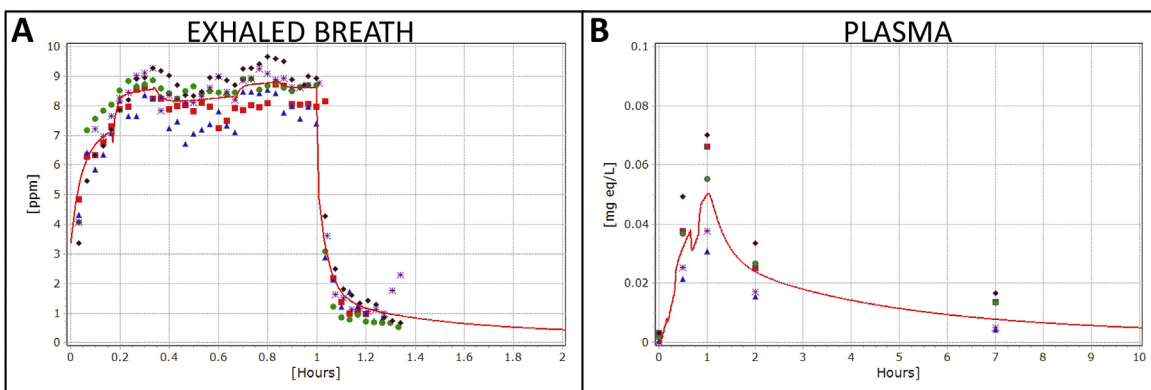
Following the parameterization of the model with select datasets, we conducted a broad evaluation of the model structure and parameters with all the available datasets to ensure that the model reproduced the time-course concentrations of both parent and total radiolabeled material in several biological matrices, including blood, tissues and exhaled breath with a single set of chemical and species specific parameters (see Results section). This approach is consistent with the recommended evaluative process to determine

the level of confidence in a PBPK model for use in risk assessment (WHO, 2010). The WHO (2010) guidance indicates that models should be evaluated on the basis of their biological plausibility, their conformance with experimental data, and the reliability of their predictions of dose metrics relevant to the intended risk assessment. Table 5 provides a summary of the characteristics of our cVMS PBPK model relevant to each of these criteria.

The integration of models under a single construct highlights the distinct attributes each cVMS have that result in chemical specific unique blood and tissue distribution. By developing a single model that incorporates key components of previous models, while also simulating the entire set of existing data equally well as did older more limited scope models, we have reduced the challenges risk assessors often face in attempting to select the most appropriate model for a risk assessment. This integrated model is sufficiently robust to derive relevant dose metrics, such as area under the curve (AUC) or peak concentration of parent material in the blood. The free concentration of parent material in the blood also provides a reasonable surrogate for target tissue dose because parent cVMSs partition fairly equally between blood and tissues, with the exception of the fat tissue. These dose metrics can be used to assess the best metric for understanding apical responses in test animals. These same dose metrics, i.e., those estimated to be best associated with outcomes in test animals, can be estimated for the expected human exposures following individual or combined dermal and inhalation exposures of workers, consumer or the general population to D4 and D5. The dose measures also become



## INHALATION



## DERMAL

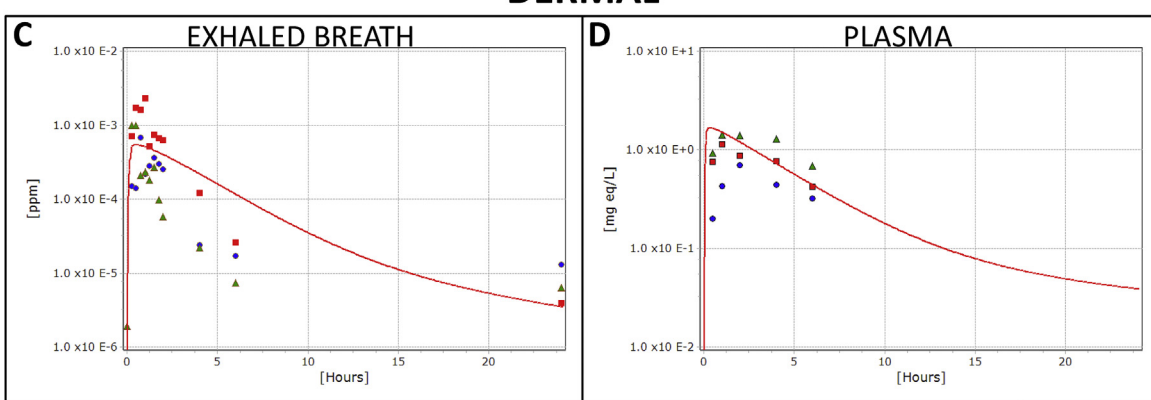


**Fig. 6.** Model simulation (lines) and data (symbols) (mean  $\pm$  SD;  $n = 3$ ) of D5 in (a) exhaled breath and (b) plasma in male volunteers during and following 10 ppm D5 vapor exposure for 1-h (c) exhaled breath and (d) plasma during and following a single application of 1.4 g  $^{13}\text{C}$ -D5 to skin axilla.

**Table 5**

Evaluation of model consistency with WHO (2010) PBPK modeling guidelines.

Key question (WHO, 2010)	D4/D5 PBPK Model	Level of confidence
Does the model structure and parameters have a reasonable biological basis?	Model structure, code and parameters have appropriate biological bases and do not violate any modeling principles or known boundary conditions for biological processes	High
How well does the PBPK model reproduce the chemical-specific PK data under various experimental or exposure conditions?	The model reproduces the important features of multiple data sets using a consistent set of species and chemical specific parameters for a variety of simulations: <ul style="list-style-type: none"> <li>• multiple dose levels</li> <li>• oral, dermal and inhalation routes of exposures</li> <li>• rodents and humans</li> </ul>	High
How reliable is the PBPK model with regard to its predictions of dose metrics relevant to risk assessment?	The model reliably reproduces the most plausible dose metric associated with hazard endpoints used in risk assessments (parent cyclic siloxane AUC in blood) in both rats and humans at relevant dose levels and relevant exposure routes for consumer protection	High

important for route-to-route, interspecies and high to low dose extrapolations for risk assessment. In this journal issue, Gentry et al. (2015) demonstrated the applicability of this integrated model in a global “harmonized” risk assessment on D5 to meet requirements for substance-specific risk assessments conducted by regulatory agencies globally.

Having one common model also allowed us to examine if there were outliers in the data or other kinetic processes that had not been adequately described with this model. This global evaluation of the datasets with a single model demonstrated that the kinetic disposition of cVMS is very consistent across dose levels, species and for both dermal and inhalation routes of exposure. Although consumers are exposed to cVMSs primarily from the dermal and inhalation routes, there is a minor contribution to total exposure via

the oral route. The kinetic dispositions of D4 and D5 were evaluated following high oral doses in various lipophilic vehicles or as neat material (Plotzke, 1998). Modeling of these data indicated that the uptake and distribution of the cVMSs following these high oral exposures in rats differed substantially from the kinetic behavior following dermal and inhalation exposures likely due to the form of the cVMSs absorbed from the GI tract in lipophilic vehicles (Saragapani et al., 2003). An oral study at more environmentally relevant exposure levels using a vehicle more consistent with a rodent food matrix was recently conducted to investigate dose and vehicle dependent kinetics (Domoradzki et al., 2015) and evaluated with a PBPK model (McMullin et al., 2015).

The concentrations of the cVMSs in the body are regulated by the low blood: air partitioning and high hepatic clearance, leading



to rapid clearance of free concentrations of D4 and D5 from the blood for both dermal and inhalation exposure. Although it takes days to weeks for D4 and D5 to reach steady state levels in the fat due to the high blood: fat partitioning, these materials are not expected to bioaccumulate in the blood or systemic tissues due to rapid clearance by other processes (exhalation due to low blood: air partitioning and high hepatic clearance due to high affinity metabolism in liver) that remove the material from the circulation. As such, rats repeatedly exposed to D4 or D5 via inhalation rapidly reach stable periodicity for plasma concentrations. Andersen et al. (2008) used a generic PBPK model to assess attributes that influence tissue concentrations of lipophilic volatile compounds and demonstrated that highly metabolized, lipophilic compounds with low blood: air partitioning, such as D5, do not accumulate in blood or systemic tissues with repeat exposures. Their conclusion was further supported by an absence of an increase in D5-tissue concentrations after a 6-month inhalation exposure during the conduct of a chronic bioassay (Jean et al., 2015; in this issue).

This integrated MC-MD model can also be used to describe the cross-species relationships between other relevant dose metrics associated with point of departures (PoDs) derived from the animal studies. These PoDs could include either parent chemical or metabolite based metrics, such as total silanols, in plasma or tissue. Importantly, there are characteristics of the rat kinetics, specifically inducible metabolism at higher D4 exposures that are not relevant for human exposures at levels much lower than those in the rat studies. Although limited biomonitoring data currently exist on the cVMS materials (Xu et al., 2012, 2015), a single model for the cVMS materials will have also applications for interpreting biomonitoring data in a risk/exposure context.

On a final note, we foresee two other contributions expected to arise from developing our integrated model. First, as data sets accumulate for other low molecular weight siloxanes, the observed kinetic behavior of these materials can be more easily compared with that seen for D4 and D5 to assess similarities or differences in the processes accounting for uptake, distribution and elimination of a wider variety of low molecular weight siloxanes. Secondly, metabolism of cVMSs and of longer chain linear siloxanes produce common silanol metabolites. With a limited suite of pharmacokinetic time course studies on specific silanols, this model could be expanded to predict these various silanols in diverse populations for any number of siloxanes.

## Appendix A. Supplementary data

Supplementary data related to this article can be found at <http://dx.doi.org/10.1016/j.yrtph.2015.12.010>.

## References

- Andersen, M.E., Reddy, M., Plotzke, K., 2008. Are highly lipophilic volatile compounds expected to bioaccumulate with repeated exposures. *Toxicol. Lett.* 179, 85–92.
- Andersen, M.E., Sarangapani, R., Reitz, R.H., Gallavan, R.H., Dobrev, I.D., Plotzke, K.P., 2001. Physiological modeling reveals novel pharmacokinetic behavior for inhaled octamethylcyclotetrasiloxane in rats. *Toxicol. Sci.* 60, 214–231.
- Brown, R.P., Delp, M.D., Lindstedt, S.L., Rhomberg, L.R., Beliles, R.P., 1997. Physiological parameter values for physiologically based pharmacokinetic models. *Toxicol. Ind. Health* 13 (4), 407–484.
- Dekant, W., Klaunig, J.E., Jul 3 2015. Toxicology of decamethylcyclopentasiloxane (D5). *Regul. Toxicol. Pharmacol.* [epub ahead of print].
- Domoradzki, J.Y., Sushynski, J., Jovanovic, M., McNett, D., Van Landingham, C., 2015. Dose-dependent disposition of 14C-Decamethylcyclopentasiloxane (D5) following oral gavage to Fisher 344 rats. In: *The Toxicologist: Supplement to Toxicological Sciences*, 144(1). Society of Toxicology. Abstract no. 2096.
- Gentry, R., Lowe, A., Van Landingham, C., Greene, T., Plotzke, K., Nov. 11 2015. A global human health risk assessment for decamethylcyclopentasiloxane (D5). *Reg. Toxicol. Pharmacol.* [epub ahead of print].
- Jean, P.A., Plotzke, K.P., Scialli, A.R., 2015. Chronic toxicity and oncogenicity of decamethylcyclotetrasiloxane in the Fischer 344 rat. *Reg. Toxicol. Pharmacol.* Jul 13 [epub ahead of print].
- Jovanovic, M.L., McMahon, J., McNett, D.A., Tobin, J.M., Plotzke, K.P., 2008. *In vitro* and *in vivo* percutaneous absorption of 14C-octamethylcyclotetrasiloxane (14C-D4) and 14C-decamethylcyclopentasiloxane (14C-D5). *Reg. Toxicol. Pharmacol.* 50 (2), 239–248.
- Looney, J.R., Utell, M.J., Plotzke, K., 2000. *In Vitro* Effects of Siloxanes on Human Immune Cells. EPA Document. F41-0102-01420.
- McMullin, T., Campbell, J., Plotzke, K.P., Andersen, M.E., Domoradzki, J.Y., Clewell, H.J., 2015. PBPK modeling describes route-specific kinetics of cyclic volatile methyl siloxanes. In: *The Toxicologist: Supplement to Toxicological Sciences*, 144(1). Society of Toxicology. Abstract no. 749.
- Plotzke, K.P., 1998. An Oral Gavage Study to Compare the Absorption Potential of 14C-octamethylcyclotetrasiloxane (D4) in Fischer 344 Rats when Delivered in Various Carriers. Dow Corning Corporation. Health and Environmental Sciences. Technical Report No. 1998-10000-44815.
- Plotzke, K.P., Crofoot, S.D., Ferdinandi, E.S., Beattie, J.G., Reitz, R.H., McNett, D.A., Meeks, R.G., 2000a. Disposition of radioactivity in Fischer 344 rats after single and multiple Inhalation Exposure to [(14C)Octamethylcyclotetrasiloxane ((14C)CJD(4))]. *Drug Metab. Dispos.* 28 (2), 192–204.
- Plotzke, K.P., Utell, M.J., Looney, J.R., 2000b. Absorption, Distribution and Elimination of 13C-d4 in Humans after Dermal Administration. EPA document. 86010000007.
- Plotzke, K.P., Utell, M.J., Looney, J.R., 2002. Absorption, Distribution and Elimination of 13C-d5 in Humans after Dermal Administration. EPA document. 84030000008.
- REACH, 2011a. Chemical Safety Report Substance Name: Decamethylcyclopentasiloxane CAS Number: 541-02-6. European Chemicals Agency (ECHA). Peter Fisk Associates Ltd, Herne Bay, United Kingdom.
- REACH, 2011b. Chemical Safety Report Substance Name: Octamethylcyclotetrasiloxane CAS Number: 556-67-2. European Chemicals Agency (ECHA). Peter Fisk Associates Ltd, Herne Bay, United Kingdom.
- Reddy, M.B., Andersen, M.E., Morrow, P.E., Dobrev, I.D., Varapath, S., Plotzke, K.P., Utell, M.J., 2003. Physiological modeling of inhalation kinetics of octamethylcyclotetrasiloxane in humans during rest and exercise. *Toxicol. Sci.* 72, 3–18.
- Reddy, M.B., Looney, R.J., Utell, M.J., Plotzke, K.P., Andersen, M.E., 2007. Modeling of human dermal absorption of octamethylcyclotetrasiloxane (D4) and decamethylcyclopentasiloxane (D5). *Toxicol. Sci.* 99, 422–431.
- Reddy, M.B., Dobrev, I.D., McNett, D.A., Tobin, J.M., Utell, M.J., Morrow, P.E., Domoradzki, J.Y., Plotzke, K.P., Andersen, M.E., 2008. Inhalation dosimetry modeling with inhaled decamethylcyclopentasiloxane in rats and humans. *Toxicol. Sci.* 105, 275–285.
- Sarangapani, R., Teeguarden, J., Andersen, M.E., Reitz, R.H., Plotzke, K.P., 2003. Route-specific differences in distribution characteristics of octamethylcyclotetrasiloxane (D4) in rats: analysis using PBPK models. *Toxicol. Sci.* 71, 41–52.
- Thrall, K.D., Soelberg, J.J., Powell, T., Corley, R.A., 2008. Physiologically based pharmacokinetic modeling of the disposition of octamethylcyclotetrasiloxane (D4) migration from implants in humans. *J. Long. Term. Eff. Med. Implants* 18, 133–144.
- Tobin, J.M., McNett, D.A., Durham, J.A., Plotzke, K.P., 2008. Disposition of decamethylcyclopentasiloxane in Fischer 344 rats following single or repeated inhalation exposure to 14C-Decamethylcyclopentasiloxane (14C-D5). *Inhal. Toxicol.* 20, 513–531.
- Utell, M.J., Gelein, R., Yu, C.P., Kenaga, C., Geigel, Torres A., Chalupa, D., Gibb, F.R., Speers, D.M., Mast, R.W., Morrow, P.E., 1998. Quantitative exposure of humans to an octamethylcyclotetrasiloxane (D4). *Vap. Toxicol. Sci.* 44, 206–213.
- Varapath, S., McMahon, J.M., Plotzke, K.P., 2003. Metabolites of hexamethyldisiloxane and decamethylcyclopentasiloxane in Fischer 344 rat urine – a comparison of a linear and a cyclic siloxane. *Drug Metab. Dispos.* 31, 206–214.
- Varapath, S., Salyers, K.L., Plotzke, K.P., Nanavati, S., 1999. Identification of metabolites of octamethylcyclotetrasiloxane (D4) in rat urine. *Am. Soc. Pharm. Exp. Ther.* 27, 1267–1273.
- World Health Organization (WHO), 2010. Characterization and Application of Physiologically Based Pharmacokinetic Models in Risk Assessment. (IPCS harmonization project document no. 9) WHO Press, Geneva, Switzerland.
- Xu, L., Shi, Y., Wang, Y., Dong, Z., Weiping, S., Cai, Y., 2012. Methyl siloxanes in environmental matrices around a siloxane production facility, and their distribution and elimination in plasma of exposed population. *Environ. Sci. Technol.* 46, 11718–11726.
- Xu, L., Shi, Y., Liu, N., Cai, Y., 2015. Methyl siloxanes in environmental matrices and human plasma/fat from both general industries and residential areas in China. *Sci. Total Environ.*